


RESEARCH

Open Access



Proposal for diagnosis using FLAIR image aimed for pediatric MELAS with recurrent stroke-like episodes on MRI system cannot take ASL imaging

Makoto Shimada^{1,2*} , Tae Ikeda³, Ryohei Fukui⁴, Katsuhiko Kida⁴, Ryutarō Matsuura⁴, Takuya Akagawa⁵ and Sachiko Goto⁴

Abstract

Background Arterial spin-labeling (ASL) imaging is currently the most useful method for diagnosing mitochondrial encephalomyopathy, lactic acidosis, and stroke-like attack syndrome (MELAS). However, ASL is often an optional feature of standard MRI systems. Therefore, not all MRI systems can perform ASL imaging. In contrast, fluid-attenuated inversion recovery (FLAIR) imaging is one of the common sequences in brain MRI because FLAIR imaging can be performed regardless of the specifications of the equipment. This study aimed to compare the diagnostic performance of quantitative analysis of signal intensity obtained from fluid-attenuated inversion recovery (FLAIR) images with ASL images for MELAS with recurrent stroke-like episodes (SLEs). A total of 68 cases with normal magnetic resonance imaging findings and 25 cases diagnosed MELAS with recurrent SLEs were included. We evaluated the frontal lobe and cuneus as target areas and compared the regional cerebral blood flow (rCBF) values obtained from ASL images with the normalized signal intensity (nSI) obtained from FLAIR images.

Results The sensitivity and specificity for diagnosing MELAS from linear discriminant analysis (LDA) obtained from the rCBF values were 0.84 and 0.941, respectively, and those of nSI were 0.8 and 0.897, respectively. The area under the ROC curves (AUC) calculated from the receiver operating characteristic (ROC) curve analysis using rCBF values and nSI were 0.889 and 0.804, respectively.

Conclusion Quantitative analysis using the signal intensity of the FLAIR image could have a diagnostic performance equivalent to that of rCBF values obtained from ASL images.

Keywords Mitochondrial encephalomyopathy lactic acidosis and stroke-like attack syndrome, Stroke-like episodes, Fluid-attenuated inversion recovery, Arterial spin labeling

Institution where the study was conducted: Osaka Women's and Children's Hospital

*Correspondence:
Makoto Shimada
itam1309@gmail.com

Full list of author information is available at the end of the article



© The Author(s) 2023. **Open Access** This article is licensed under a Creative Commons Attribution 4.0 International License, which permits use, sharing, adaptation, distribution and reproduction in any medium or format, as long as you give appropriate credit to the original author(s) and the source, provide a link to the Creative Commons licence, and indicate if changes were made. The images or other third party material in this article are included in the article's Creative Commons licence, unless indicated otherwise in a credit line to the material. If material is not included in the article's Creative Commons licence and your intended use is not permitted by statutory regulation or exceeds the permitted use, you will need to obtain permission directly from the copyright holder. To view a copy of this licence, visit <http://creativecommons.org/licenses/by/4.0/>.

Background

Mitochondrial encephalomyopathy, lactic acidosis, and stroke-like attack syndrome (MELAS) are common clinical forms of mitochondrial disease, a multisystem disorder that occurs in childhood in approximately 70% of cases [1–3]. MELAS is characterized by stroke-like episodes (SLEs), such as headache, vomiting, convulsions, impaired consciousness, and motor paralysis of the extremities [4]. A typical MELAS lesion is an edematous lesion centered in the cerebral cortex that is not consistent with vascular control areas [5]. SLE lesions often appear from the unilateral cuneus to the temporal lobe, and distinguishing MELAS from cerebral infarction is important. SLE lesions appear as high-signal areas on diffusion-weighted images; however, the apparent diffusion coefficient values of SLE lesions do not show a strongly decreased intensity area compared with cerebral infarctions. MELAS is often associated with dilated vessels due to vascular endothelial dysfunction, resulting in foci of predominantly vasogenic edema due to extravasation [6]; however, in the subacute phase, there may also be a mixture of cytotoxic edema in the foci. Arterial spin labeling (ASL) imaging is currently the most useful imaging for differentiating MELAS from cerebral infarction because it can easily capture increased blood flow at SLE lesions [7, 8]. ASL uses an inversion pulse to magnetically label the arterial blood flowing into the imaging cross section, which is then used as a tracer [9], and a labeling pulse is applied. It is a non-invasive imaging method that measures brain perfusion by collecting data after a delay time between the application of the labeling pulse, called post-labeling delay, and data collection. Recently, magnetic resonance imaging (MRI) has seen rapid technological advances in pulse sequencing and the proliferation of hardware, such as high-field devices and high-sensitivity phased array coils. However, ASL is often an optional feature of standard MRI systems. Therefore, not all MRI systems can perform ASL imaging. In contrast, fluid-attenuated inversion recovery (FLAIR) imaging is one of the common sequences in brain MRI because FLAIR imaging can be performed regardless of the specifications of the equipment [10, 11]. FLAIR is an imaging technique that suppresses the cerebrospinal fluid signal by scanning at a time when the longitudinal magnetization of the cerebrospinal fluid becomes negative when a 180° inversion pulse is applied and then returns to zero. FLAIR is characterized by lesions in contact with cerebrospinal fluid, such as the cortex and periventricular walls, which are more easily visualized than T2-weighted imaging. This study aimed to compare the diagnostic performance of quantitative analysis of signal intensity obtained from FLAIR images with ASL images for MELAS with recurrent SLEs.

Methods

Subjects

Sixty-eight cases were included as the normal group, as they were diagnosed with normal findings and without developmental delay or organic abnormalities in the brain parenchyma on MRI. Additionally, 25 cases diagnosed MELAS with recurrent SLEs were included as the MELAS group. The normal group included 28 males and 40 females with a median age of 8.5 years (range 5 months to 14 years). The MELAS group included 25 females with a median age of 11.17 years (range 9–14 years). All cases underwent ASL and FLAIR imaging on brain MRI scans from May 2015 to May 2021 in our hospital. All cases underwent MRI examination with closed eyes.

Image acquisition

MRI images were obtained using an Optima 450w 1.5T scanner (GE Healthcare, Milwaukee, WI, USA). A 16-channel GEM Head Neck Unit coil was used as the receiving coil. The imaging parameters of the ASL and FLAIR images are listed in Table 1.

Regional cerebral blood flow calculation

The frontal lobe and cuneus were evaluated as target areas at the basal ganglia level on transverse ASL images. As aforementioned, we chose the cuneus as the target area because of the increased blood flow in the cuneus in MELAS cases. The frontal lobe was selected because it is the region furthest from the cuneus. The console attached to the MRI scanner was used to locate three circular regions of interest (ROIs), each 50 mm² in size, on both sides of the frontal lobe and cuneus. Regional cerebral blood flow (rCBF) was measured in

Table 1 Imaging parameters of ASL and FLAIR images

Image	ASL (pulsed continuous ASL)	FLAIR
Dimension	3D	2D
Pulse sequence	fast spin echo	fast spin echo
Slice plane	Axial	Axial
TR [msec]	4555	9000
TE [msec]	10.7	120
TI [msec]	-	2500
RFA [°]	-	160
FOV [mm]	220	220
Matrix	-	320 * 192
Points * Arms	512 * 6	-
Slice thickness [mm]	4	6
NEX	2	1
Band width [kHz]	± 62.5	± 31.25
PLD [msec]	1525	-
Labeling duration [msec]	1450 (fixed)	-
Scan time [sec]	146	189

the ROIs, and the mean value of rCBF obtained from the six ROIs was used in the analysis (Fig. 1). This procedure was performed in all cases in the normal and MELAS groups.

Signal intensity of FLAIR images

The frontal lobe and cuneus on transverse FLAIR images were also evaluated as well as ASL images. A circular ROI of 200 mm² and oval ROI of 200 mm² were located on each side of the frontal lobe and cuneus, respectively (Fig. 2a). The signal intensity in the ROIs was measured, and the mean signal intensity was calculated. However, the signal intensities of the frontal lobe and cuneus obtained from the FLAIR images were relative values, unlike rCBF, which is an absolute value. Therefore, the mean signal intensity was normalized to the signal intensity in the brainstem. This is referred to as the normalized signal intensity (nSI). A 180-mm² circular ROI was located on the brainstem to avoid the effect

of cerebrospinal fluid on signal intensity, and the signal intensity in the ROI was averaged for normalization (Fig. 2b).

Statistical analysis

Spearman's rank correlation coefficient was calculated using the rCBF values and nSI obtained from the frontal lobe and cuneus in all cases [12]. To distinguish between the normal and MELAS groups, linear discriminant analysis (LDA) was performed to obtain the linear decision boundary, which was estimated from a scatter plot of the rCBF values and nSI. Fisher's method was employed to analyze LDA results [13]. The sensitivity and specificity were determined using these decision boundaries. Additionally, receiver operating characteristic (ROC) curves and the area under the ROC curve (AUC) were estimated using the rCBF values and nSI in the frontal lobe and cuneus. The DeLong method was employed for statistical analysis of the two AUCs

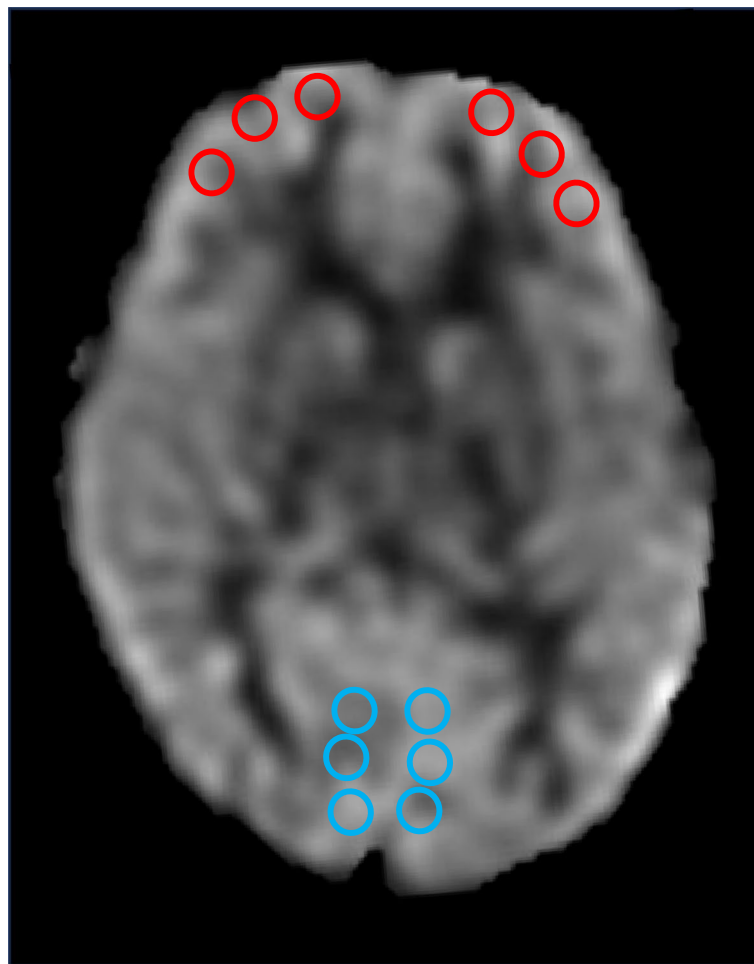


Fig. 1 Locations of 12 ROIs in the frontal lobe and cuneus for measuring rCBF values using ASL images. Each circular ROI has an area of 50 mm²

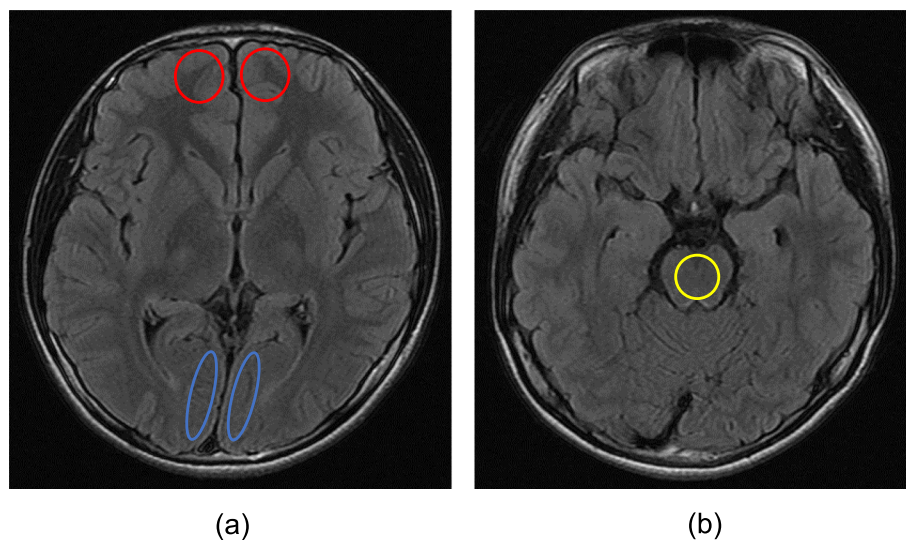


Fig. 2 Location of the ROI of the frontal lobe, cuneus, and brainstem for measuring normalized signal intensity using FLAIR images. **a** The circle ROI of the frontal lobe has an area of 200 mm². The oval ROI of the cuneus has an area of 200 mm². **b** The circle ROI of the brainstem has an area of 180 mm²

to compare the diagnostic performance of the imaging modalities for MELAS [14]. We used R Studio (version 2023.06.1+524, posit, Boston, USA) to perform the statistical analysis, with a significance level of 0.05.

Results

The correlation coefficients of rCBF values for the frontal lobe and cuneus in the normal and MELAS groups were 0.47 and 0.46, respectively. Those of nSI were 0.871 and 0.746, respectively. Scatter plots of the rCBF values and nSI for the normal and MELAS groups are shown in Figs. 3 and 4. We also show the decision boundaries estimated from LDA, distinguishing between the normal and MELAS groups. From the decision boundaries of rCBF values, the sensitivity and specificity for the diagnosis of MELAS were 0.84 and 0.941, respectively, and those of nSI were 0.8 and 0.897, respectively (Table 2).

The four clinical images diagnosed MELAS are shown in Fig. 5. In the positive case diagnosed with MELAS, based on the decision boundaries obtained from the LDA of the rCBF values, there was a clear increase in blood flow from the right cuneus to the temporal lobe (Fig. 5a). In the positive case diagnosed with MELAS from the LDA of nSI, there was a clear T2 prolongation area in the right occipital lobe and from the left cuneus to the left temporal lobe, and increased blood flow on ASL images consistent with the same area (Fig. 5b). In the case that was not distinguished as MELAS using the decision boundaries obtained from the rCBF values

and nSI, the right cuneus to the right occipital lobe was the site of the lesion; however, there was no obvious increase in blood flow and area of T2 prolongation (Fig. 5c). In the case of MELAS diagnosed on the border of the decision boundary obtained from the LDA of nSI, the right cuneus to the right temporal lobe was the site of the lesion, but there was no obvious T2 prolongation area, while ASL images showed an obvious increase in blood flow in the same area (Fig. 5d). The AUCs for the ASL and FLAIR images were 0.889 and 0.804, respectively, as estimated from the ROC curves using the rCBF values and nSI (Fig. 6). There was no significant difference between the two AUC values ($p = 0.173$).

Discussion

In this study, we examined the clinical utility of FLAIR imaging for the diagnosis of MELAS with recurrent SLEs compared to ASL imaging. The results showed that the rCBF values obtained from ASL images and the nSI obtained from FLAIR images were equivalent to their diagnostic performance in MELAS cases. We calculated Spearman's rank correlation coefficient using the rCBF values and found no correlation between the normal and MELAS groups. We considered that the degree of increased blood flow in recurrent SLEs varied by case. However, as shown in Fig. 3, the overall rCBF values were higher in the MELAS cases than in the normal cases, especially in the cuneus. Therefore, only the

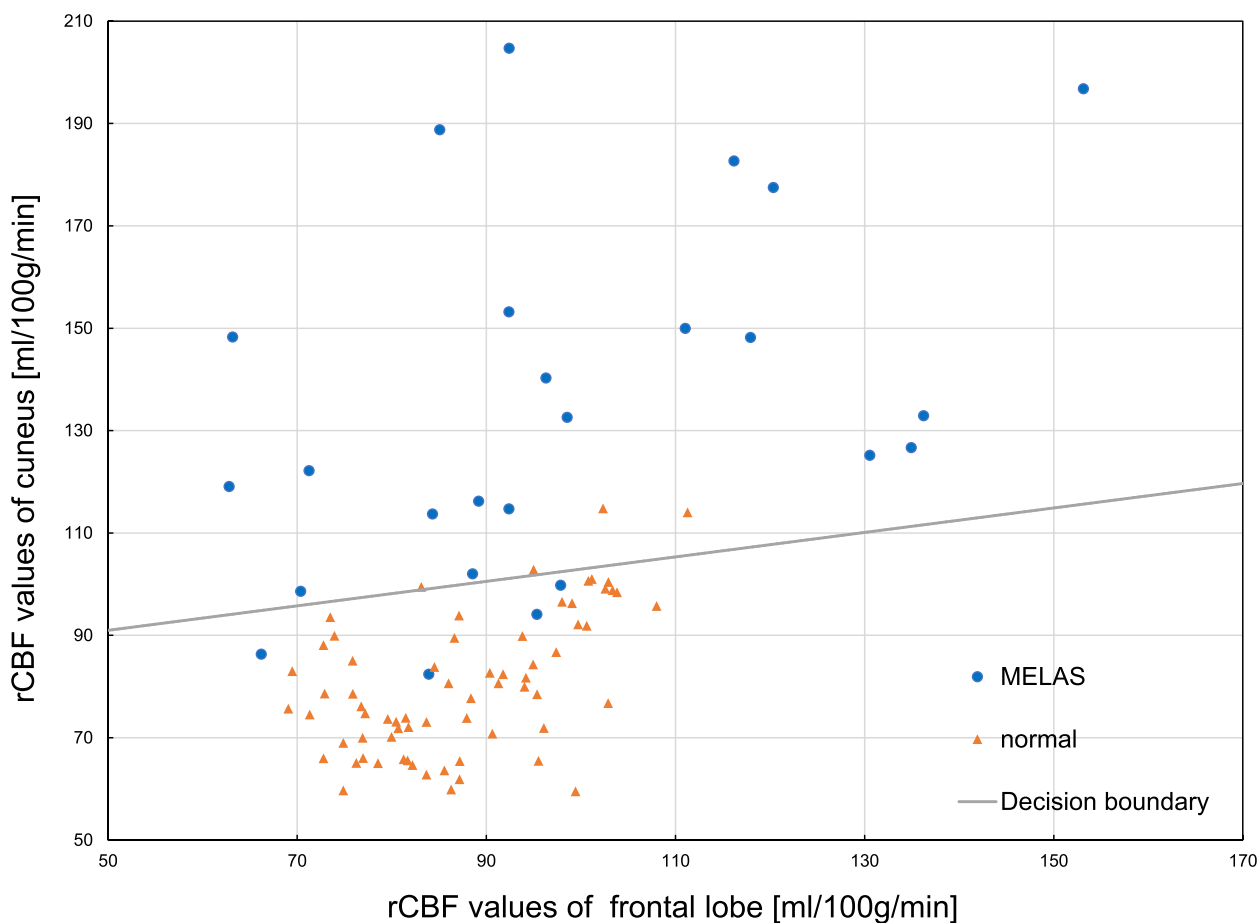


Fig. 3 Results of rCBF values obtained from ASL images and the decision boundary calculated using LDA

degree of increased blood flow can easily indicate an abnormality of the brain; this is consistent with findings of previous reports [7, 8]. In contrast to the rCBF values, there was a strong positive correlation in the nSI results. The high correlation of the nSI obtained from FLAIR images is due to the smaller signal intensity in MELAS cases and normalization of the signal intensity by dividing it by the signal intensity of the brainstem. We considered that the correlation coefficient of nSI was also higher because normalization allowed the variation in signal values to be compared between cases. Based on the decision boundaries obtained from LDA, both the sensitivity and specificity for diagnosing MELAS using the rCBF value were higher than those of the nSI; however, there were few differences. Regarding sensitivity, in the positive cases diagnosed with MELAS on the border of the decision boundary obtained from the LDA of nSI, one MELAS-positive case could be distinguished by the ASL image, which

was the cause for the slight difference. We considered that the difference in specificity was due to the larger rCBF values of cuneus in MELAS cases than in normal cases, and the smaller signal intensity in MELAS cases and the smaller difference between MELAS and normal cases. Care must be taken in cases of MELAS that cannot be distinguished using either rCBF values or nSI. In this study, MRI examination of recurrent SLEs was performed; however, there were no abnormalities on the ASL or FLAIR images (Fig. 5c). Li et al. reported that persistent cellular injury due to impaired adenosine triphosphate production may give rise to excessive loss of neurons, resulting in decreased rCBF in the affected brain regions during the chronic phase of SLEs [7]. Therefore, our method is not appropriate for these cases, and we need to perform a comprehensive diagnosis in conjunction with physical findings and other examination results. We calculated AUC values from ROC analysis using rCBF values and the nSI, and

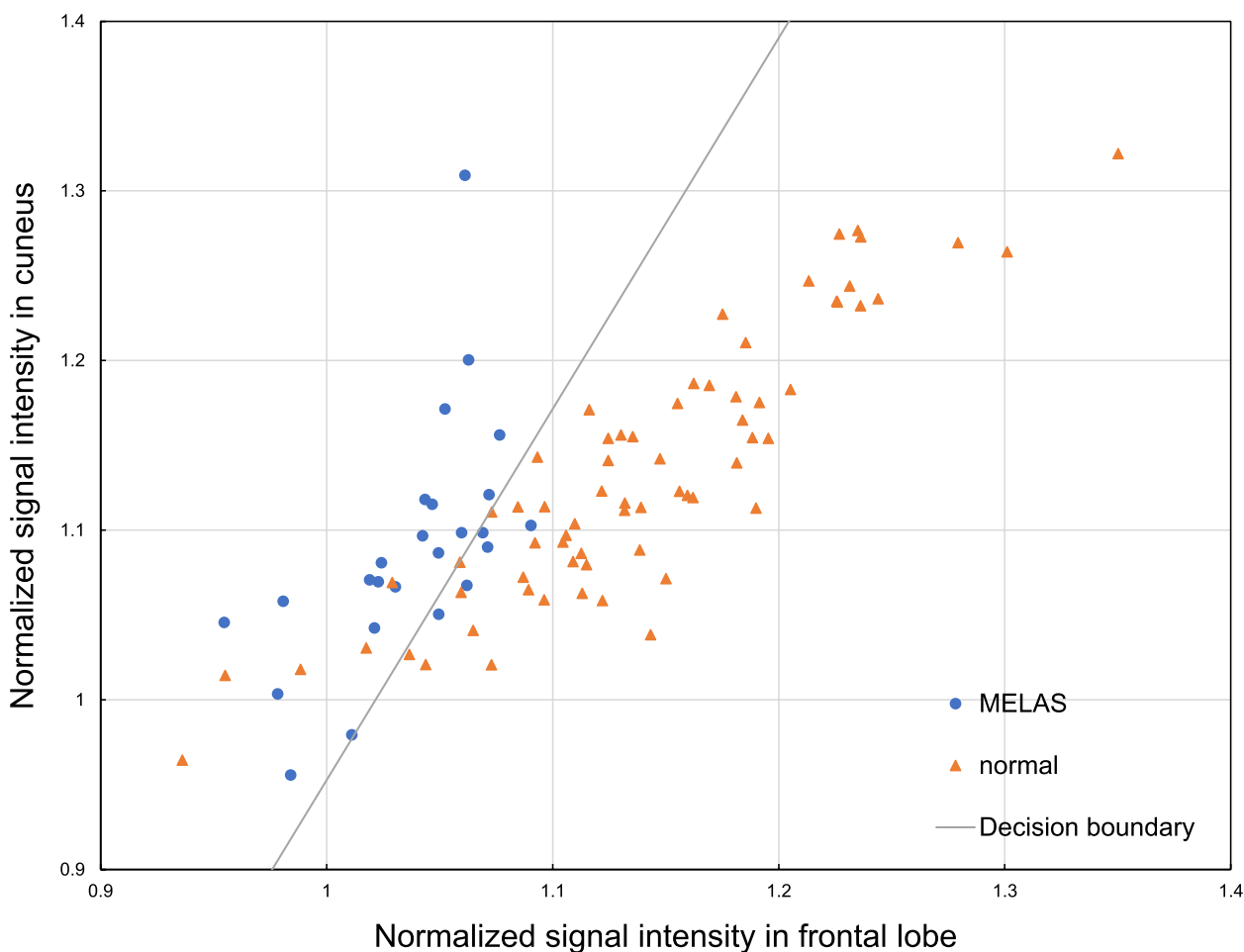


Fig. 4 Results of the normalized signal intensity obtained from FLAIR images and the decision boundary

Table 2 Sensitivity and specificity for MELAS cases obtained from the LDA

Image	Sensitivity	Specificity
ASL (n=93)	0.84 (21/25)	0.941 (64/68)
FLAIR (n=93)	0.8 (20/25)	0.897 (61/68)

recognized that ASL images have better diagnostic performance than FLAIR images.

However, there was no statistically significant difference between the AUC values obtained from the ASL and FLAIR images. On the basis of the results, we concluded that the diagnostic performances of ASL and FLAIR images for MELAS with recurrent SLEs were equivalent using our method.

Edematous lesions with cortical predominance may persist long after symptom resolution, although FLAIR high-signal lesions may shrink in size. Using this method, it is possible to determine whether SLEs have recurred in residual FLAIR high-signal lesions that are difficult to assess visually. In addition, although the cases in this study were obtained at the time of recurrent SLEs, a case was reported in which ASL image over time captured increased blood flow in the preictal lesion, and it was also reported that ASL imaging was useful in predicting seizures [15, 16]. If our method has a diagnostic performance equivalent to that of ASL imaging, we suggest that FLAIR imaging may also be useful in predicting seizures.

A limitation of this study was the small number of MELAS cases; however, we considered that a population trend was obtained when considering the distribution of the scatter plots. In addition, both angioedema and cellular edema show high signal intensity on FLAIR images

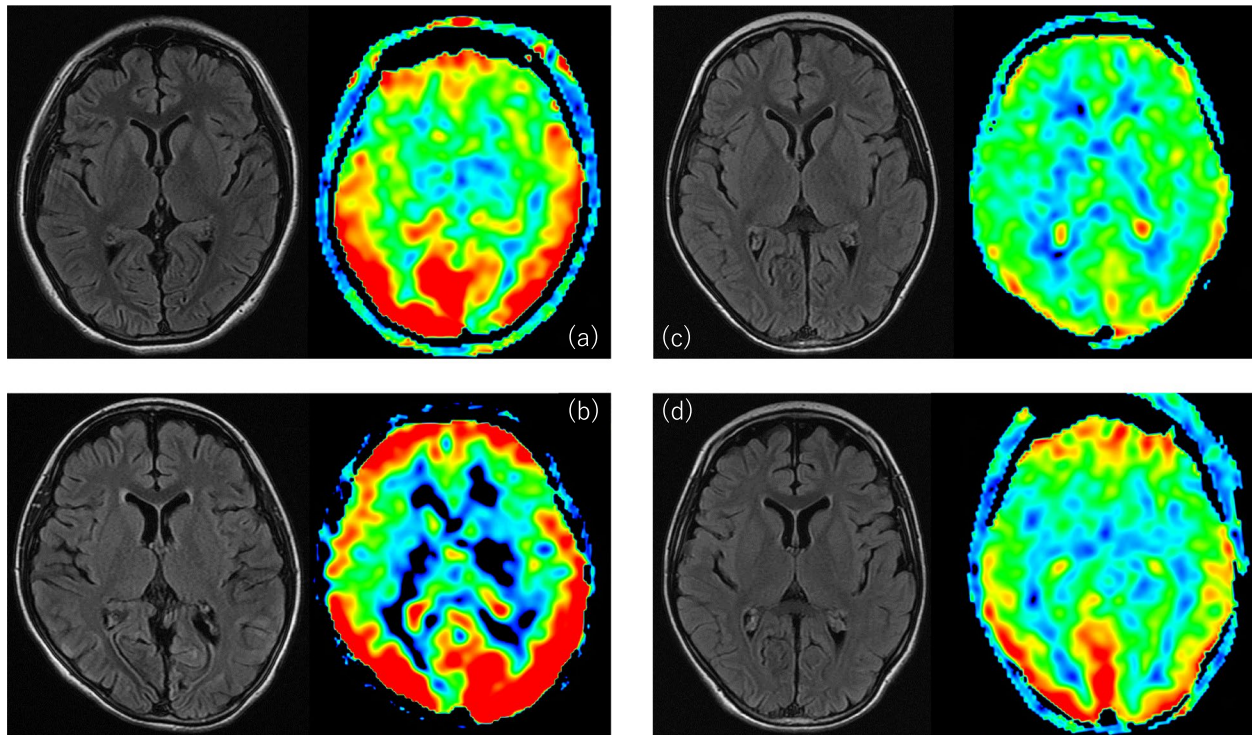


Fig. 5 MELAS cases analyzed in this study. Positive cases were determined by the decision boundary obtained from the **a** rCBF value and **b** nSI. **c** Cases in which MELAS could not be diagnosed using rCBF or nSI. **d** Case located on the decision boundary obtained from nSI

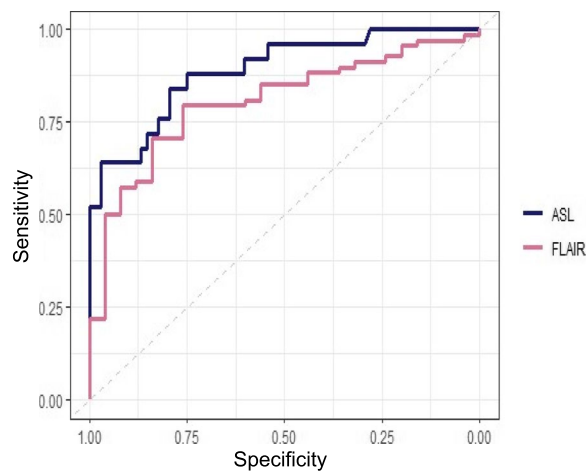


Fig. 6 ROC curves for diagnosing MELAS by using the ASL and FLAIR images

and may not be discriminated based solely on the signal intensity of the FLAIR image. Thus, we consider that the diagnosis of such cases should be proceeded with other sequences.

Conclusions

Quantitative analysis of the signal intensity in FLAIR images had a diagnostic performance equivalent to that of the rCBF values obtained from ASL images when diagnosing MELAS with recurrent SLEs. Using our method, MELAS can be diagnosed even in facilities with MRI system that cannot perform ASL imaging.

Abbreviations

MELAS	Mitochondrial encephalomyopathy lactic acidosis and stroke-like attack syndrome
SLEs	Stroke-like episodes
ASL	Arterial spin labeling
MRI	Magnetic resonance imaging
FLAIR	Fluid-attenuated inversion recovery
ROI	Regions of interest
rCBF	Regional cerebral blood flow
nSI	Normalized signal intensity
LDA	Linear discriminant analysis
AUC	Area under the ROC curve

Authors' contributions

MS designed the study, collected and analyzed the data, and wrote this manuscript. TI performed data collection, analysis, and paper review. RF provided data analysis methodology. KK, RM, TA, and SG discussed the results of the analysis and checked the text of this paper.

Availability of data and materials

The datasets generated and/or analyzed during the current study are not publicly available due [REASON WHY DATA ARE NOT PUBLIC] but are available from the corresponding author on reasonable request.

Declarations

Ethics approval and consent to participate

The study protocol and use of clinical images were approved by the Ethical Review Committee of Osaka Women's and Children's Hospital (approval number: 1356).

Consent for publication

Not applicable.

Competing interests

The authors declare that they have no competing interests.

Author details

¹Faculty of Health Sciences Graduate School of Health Sciences, Okayama University, Okayama Daigaku Igakubu Hoken Gakka Daigakuin Hokengaku Kenkyuka, 2-5-1, Shikata-cho, Kita-ku, Okayama 700-8558, Japan. ²Department of Radiology, Osaka International Cancer Institute, 3-1-69Chuo-ku, OtemaeO-saka 541-8567, Japan. ³Department of Pediatric Neurology, Kitakyushu City Yahata Hospital, 2-6-2Yahatahigashi-ku, OguraKitakyushu, Fukuoka 805-8534, Japan. ⁴Department of Radiological Technology, Faculty of Health Sciences, Okayama University, 2-5-1, Shikata-cho, Kita-ku, Okayama 700-8558, Japan. ⁵Department of Radiological Technology, Tokushima Red Cross Hospital, 103, Irinokuchi, Komatsushima-cho, Komatsushima, Tokushima 541-8567, Japan.

Received: 16 October 2023 Accepted: 23 October 2023

Published online: 13 November 2023

References

1. Yatsuga S, Povalko N, Nishioka J, Katayama K, Kakimoto N, Matsuishi T, Kakuma T, Koga Y; Taro Matsuoka for MELAS Study Group in Japan (2012) MELAS: a nationwide prospective cohort study of 96 patients in Japan. *Biochim Biophys Acta* 1820:619–624
2. Hirano M, Pavlakis SG (1994) Mitochondrial myopathy, encephalopathy, lactic acidosis, and stroke-like episodes (MELAS) current concepts. *J Child Neurol* 9:4–13
3. Sproule DM, Kaufmann P (2008) Mitochondrial encephalopathy, lactic acidosis, and stroke-like episodes: basic concepts, clinical phenotype, and therapeutic management of MELAS syndrome. *Ann NY Acad Sci* 1142:133–158
4. El-Hattab AW, Adesina AM, Jones J, Scaglia F (2015) MELAS syndrome: clinical manifestations, pathogenesis, and treatment options. *Mol Genet Metab* 116(1–2):4–12
5. Iizuka T, Sakai F, Suzuki N, Hata T, Tsukahara S, Fukuda M, Takiyama Y (2002) Neuronal hyperexcitability in stroke-like episodes of MELAS syndrome. *Neurology* 59:816–824
6. Yoneda M, Maeda M, Kimura H, Fujii A, Katayama K, Kuriyama M (1999) Vasogenic edema on MELAS: a serial study with diffusion-weighted MR imaging. *Neurology* 53:2182–2184
7. Li Rui HF, Xiao JH, Lyu J J, Wang D, Ma L, Lou X, 2017 Differential diagnosis of mitochondrial encephalopathy with lactic acidosis and stroke-like episodes (MELAS) and ischemic stroke using 3D pseudocontinuous arterial spin labeling *J Magn Reson Imaging* 45 199–206
8. Li X, Wang Y, Wang Z, Lu J, Xu Y, Ye J, Kuang Z, Li B, Pan M, Chen W, Lu S, Zhou Z, Cheng L, Wang H (2018) Comparison of magnetic resonance spectroscopy (MRS) with arterial spin labeling (ASL) in the differentiation between mitochondrial encephalomyopathy, lactic Acidosis, plus stroke-like episodes (MELAS) and acute ischemic stroke (AIS). *J Clin Neurosci* 55:65–70
9. Detre JA, Leigh JS, Williams DS, Koretsky AP (1992) Perfusion imaging. *Magn Reson Med* 23:37–45
10. De Coene B, Hajnal JV, Gatehouse P, Longmore DB, White SJ, Oatridge A, Pennock JM, Young IR, Bydder GM (1992) MR of the brain using fluid-attenuated inversion recovery (FLAIR) pulse sequences. *AJNR Am J Neuroradiol* 13:1555–1564
11. Oatridge A, Hajnal JV, Cowan FM, Baudouin CJ, Young TR, Bydder GM (1993) MRI diffusion-weighted imaging of the brain: contributions to image contrast from CSF signal reduction, use of a long echo time and diffusion effects. *Clin Radiol* 47:82–90
12. Spearman C (1910) Correlation calculated from faulty data. *Br J Psychol* 3:1–62
13. Fisher RA (1936) The use of multiple measurements in taxonomic problems. *Annals of Eugenics* 7:179–188
14. DeLong ER, DeLong DM, Clarke-Pearson DL (1988) Comparing the areas under two or more correlated receiver operating characteristic curves: a nonparametric approach. *Biometrics* 44:837–845
15. Ikawa M, Yoneda M, Muramatsu T, Matsunaga A, Tsujikawa T, Yamamoto T, Kosaka N, Kinoshita K, Yamamura O, Hamano T, Nakamoto Y, Kimura H (2013) Detection of preclinically latent hyperperfusion due to stroke-like episodes by arterial spin-labeling perfusion MRI in MELAS patients. *Mitochondrion* 13:676–680
16. Li Y, Lin J, Sun C, Zhao C, Li H (2017) Increased cerebral blood flow as a predictor of episodes in MELAS using multimodal MRI. *J Magn Reson Imaging* 46:915–918

Publisher's Note

Springer Nature remains neutral with regard to jurisdictional claims in published maps and institutional affiliations.

Submit your manuscript to a SpringerOpen[®] journal and benefit from:

- Convenient online submission
- Rigorous peer review
- Open access: articles freely available online
- High visibility within the field
- Retaining the copyright to your article

Submit your next manuscript at ► [springeropen.com](https://www.springeropen.com)